On the Temperature Behavior of Hot-Carrier Degradation

S. Tyaginov*,†, M. Jech*, P. Sharma*, J. Franco°, B. Kaczer°, and T. Grasser*
*Institute for Microelectronics, Vienna University of Technology, Gußhausstraße 27-29, A-1040 Wien, Austria
†Ioffe Physical-Technical Institute, Polytechnicheskaya 26, 194021 St-Petersburg, Russia
° imec, Kapeldreef 75, 3001 Leuven, Belgium
Email: tyaginov@iue.tuwien.ac.at

***Abstract*—We show that – in contrast to previous findings – hot-carrier degradation (HCD) in scaled nMOSFETs with a channel length of 44 nm appears to be weaker at elevated temperatures. However, the distance between degradation traces obtained at 25 and 75° C reduces as the stress voltages increase and at a certain voltage the changes of the linear drain current measured at 25 and 75° C are almost identical in the entire stress time window. We apply our physics-based model for hot-carrier degradation to analyze the temperature behavior of this detrimental phenomenon. This behavior is interpreted in terms of competing single- and multiple-carrier processes of Si-H bond dissociation with the corresponding rates having the opposite temperature dependencies. One of the most important aspects relevant to the temperature behavior of HCD is the bond vibrational life-time which decreases with the temperature.**

I. Introduction

The current understanding of hot-carrier degradation (HCD) suggests the change of the dominant mechanism which triggers HCD as transistor dimensions scale down [1–6]. In short-channel MOSFETs HCD is assumed to be driven by the multiple-carrier process of Si-H bond dissociation, while in longer devices with higher operating/stress voltages bond-breakage is typically dominated by the single-carrier process. For the first mechanism, bond-breakage occurs via the multiple vibrational excitation (MVE) of the bond by several particles subsequently bombarding the bond. On the other hand, the single-carrier mechanism relies on the interaction of a solitary hot carrier with the bond. Such a carrier can excite one of the bonding electrons to an antibonding (AB) state, thereby triggering hydrogen release. Therefore, the latter process is only probable when hot carriers are available in sufficient numbers, i.e. in the case of high stress/operating voltages.

However, we have recently shown [7–9] that the AB-process can still play an important role even in short-channel transistors, while the MVE-mechanism can be prominent in high-voltage devices as well. Such a trend has also been independently reported by Bravaix's group [10]. This behavior can be explained by a strong coupling of the MVE- and AB-mechanisms [5, 11]. According to this bond-breakage scenario, first the Si-H bond is heated by carriers with energies lower than the threshold energy needed for triggering an AB-event. If the bond is excited, the AB-process activation energy is reduced, and therefore the probability to find an electron with an energy above the threshold for this bond dissociation reaction is higher.

The interplay between the AB- and MVE-processes determines the temperature behavior of HCD which is intricate. It is worth emphasizing that this behavior is channel length dependent. In long-channel MOSFETs, scattering mechanisms such as electron-phonon interactions, scattering at ionized impurities, surface scattering, etc., suppress the high energetical fraction of the carrier packet. These processes have higher rates at elevated temperatures and therefore the high-energy tails of the carrier energy distribution function are depopulated more efficiently. If HCD is dominated by the AB-process, the change of the device characteristics appears to be less pronounced. This is typical for long-channel and/or high-voltage devices [12, 13]. Note also that in scaled MOSFETs the high-energy carrier fraction can be more populated at higher temperature due to electron-electron scattering [2, 5, 9, 11, 14, 15]. As a result, the AB-process rate can also become higher at elevated temperatures. This scenario is typical for MOSFETs with channel lengths shorter than about hundred nanometers [15], where EES plays a substantial role, thereby enhancing HCD at higher temperatures [16, 17].

As for the MVE-process, the situation is more complex. First, just like the AB-process, the rate of this mechanism is determined by the shape of the carrier energy distribution function (DF) [5, 11]. However, the threshold energy for multiple excitations of the bond corresponds to the distance between the bond eigenstates $\hbar\omega$ and thus is much lower than the bond-breakage energy [3, 18]. Therefore, one may expect that the dominant contribution to the MVE-process rate is provided by carriers with low and moderate energies. For these energies the DF values can be lower at elevated temperatures. Second, hydrogen activation over the potential barrier which separates a bonded state and the transport mode is modeled by an Arrhenius-like rate which increases with temperature (T).

Another very important factor which impacts the HCD temperature behavior is the Si-H bond vibrational life-time τ_{e}. This life-time is a decreasing function of T [19, 20]. Thus, at elevated temperatures the vibrational modes decay faster and hence the excited levels of the bond are less populated and MVE-process becomes less severe. Since – as we have shown in [5, 7, 8] – the AB- and MVE-processes are strongly coupled, a change in the τ_{e} value can dramatically affect the bond rupture rate.

Summarizing all this, we conclude that in short-channel MOSFETs the temperature behavior can be quite complex due to the interplay of several factors. In this paper, we apply our physics-based HCD model [5, 11] to describe the HCD temperature behavior in scaled nMOSFETs with a channel length of 44 nm. Stress voltages have been chosen high enough to ensure a substantial contribution of both AB- and MVE-processes [5, 11]. We show that even if the gate length is fixed,

978-1-4673-7396-8/15/$31.00 ©2015 IEEE

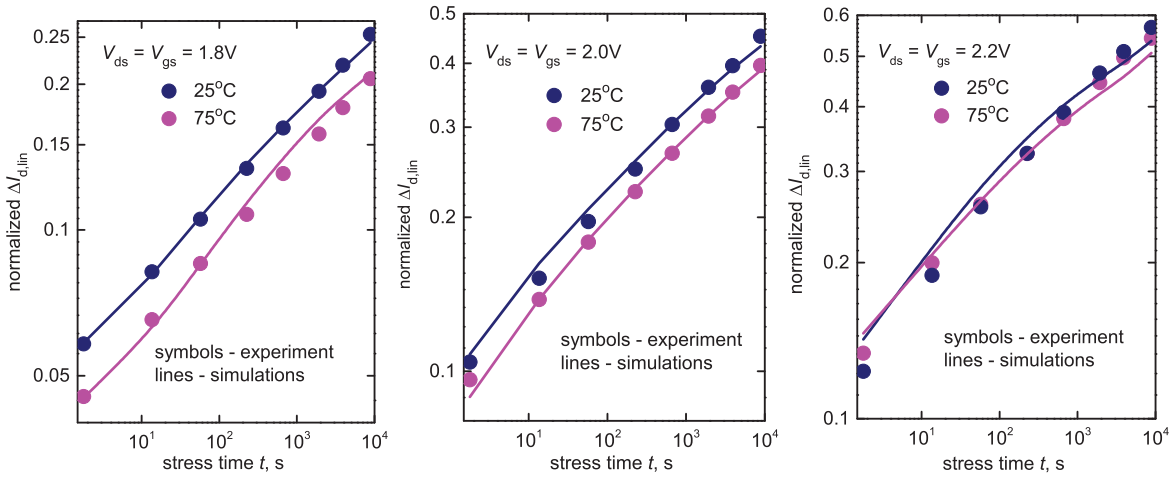

Fig. 1. The experimental changes of the linear drain current as a function of stress time $\Delta I_{\rm dlin}(t)$ plotted vs. simulated ones for three different combinations of stress voltages ($V_{\rm ds}$ = $V_{\rm gs}$ = 1.8, 2.0, and 2.2 V) and two different temperatures, 25 and 75° C. One can see that the distance between the $\Delta I_{\rm dlin}(t)$ curves obtained for 25 and 75° C decreases as $V_{\rm ds}$, $V_{\rm gs}$ increase. For $V_{\rm ds}$ = $V_{\rm gs}$ = 2.2 V, however, the $\Delta I_{\rm dlin}$ values are almost the same in the entire stress time window. The agreement between the experimental and simulated $\Delta I_{\rm dlin}(t)$ data is very good.

the temperature behavior of hot-carrier degradation can change as the stress voltage increases.

II. Experiment

nMOSFETs with a 2.5 nm thick SiON layer (grown by a decoupled plasma nitridation process) and an effective channel length of 44 nm (the gate length is 65 nm) were subjected to hot-carrier stress at the worst-case conditions for these scaled devices, i.e. at equal drain ($V_{\rm ds}$) and gate ($V_{\rm gs}$) voltages. Different combinations of stress biases were used, namely $V_{\rm ds}$ = $V_{\rm gs}$ = 1.8, 2.0, and 2.2 V, and at two different temperatures, 25 and 75° C. The linear drain current change $\Delta I_{\rm dlin}$ as a function of stress time t was recorded up to ∼9 ks, see Fig. 1.

Although experimental data published for scaled devices – i.e. with a channel length shorter than ∼100 nm – suggest that HCD is more severe at higher temperatures [2, 16, 17], Fig. 1 shows that $\Delta I_{\rm dlin}$ measured at 25° C is higher than at 75° C for $V_{\rm ds}$ = $V_{\rm gs}$ = 1.8 and 2.0 V. However, the distance between the $\Delta I_{\rm dlin}(t)$ curves decreases as the stress voltages $V_{\rm ds}$, $V_{\rm gs}$ increase and in the case of $V_{\rm ds}$ = $V_{\rm gs}$ = 2.2 V, the linear drain current change is almost the same for both temperatures in the whole stress time window.

III. The Modeling Framework

Our physics-based HCD model is implemented in the deterministic Boltzmann transport equation solver ViennaSHE [21, 22]. ViennaSHE calculates the carrier distribution functions for given stress conditions which are then used to evaluate the Si-H bond-breakage rates [5, 11]. We consider all possible superpositions of the MVE- and AB-processes. This means that bond rupture induced by the AB-process can occur not only from the ground state but also from an excited level E_i if the bond was pre-heated due to subsequent bombardment of several lower energetic carriers. The rates of both AB- and MVE-processes are determined by the carrier acceleration integral which is defined as $I = \int f(E)g(E)v(E)\sigma(E){\rm d}E$, where $f(E)g(E)$ is the generalized DF (i.e. the occupation number multiplied by the density-of-states), $v(E)$ the carrier velocity, while $\sigma(E)$ is the reaction cross section.

To describe the bond-breakage kinetics we use the truncated harmonic oscillator model of the Si-H bond. The depth of the oscillator quantum well corresponds to the bond-breakage energy $E_{\rm a}$. This energy also enters the Keldysh-like reaction cross section for the AB-process, which is modeled as $\sigma_{\rm AB}(E) = \sigma_{\rm AB,0}(E - E_{\rm a} + E_i + d \times F_{\rm ox})^{\rm p_{AB}}$ with the prefactor $\sigma_{\rm AB,0}$ being the cross section. The term $d \times F_{\rm ox}$ represents the reduction of the bond-breakage energy due to the interaction of the bond dipole moment d with the oxide electric field $F_{\rm ox}$ [5, 11, 18, 23]. In the case of the MVE-process the bond excitation/de-excitation rates are obtained as $P_{\rm u} = 1/\tau_{\rm e} \times \exp(-\hbar\omega/kT) + I_{\rm MVE}$ and $P_{\rm d} = 1/\tau_{\rm e} + I_{\rm MVE}$, where $\hbar\omega$ is the distance between the oscillator levels, $\tau_{\rm e}$ the vibrational life-time, and k the Boltzmann constant. The reaction cross section for this process is $\sigma_{\rm MVE}(E) = \sigma_{\rm MVE,0}(E - \hbar\omega)^{\rm p_{MVE}}$, where the prefactor $\sigma_{\rm MVE,0}$ is the cross section. There are two different vibrational excitation types of the Si-H bond, i.e. the bending mode and the stretching mode [18, 24, 25]. The distance between the bond eigenstates and the bond-breakage energy of the former mode are $\hbar\omega$ = 0.075 eV and $E_{\rm a}$ = 1.5 eV. In the case of the latter one these parameters are $\hbar\omega$ = 0.25 eV and $E_{\rm a}$ = 2.5 eV.

In the previous version of our model [11, 22], as well as in the model developed by Bravaix's group [3, 18], it is assumed that breakage of the Si-H bond occurs via the bending mode. However, electron paramagnetic resonance studies have shown that the activation energy for the depassivation reaction from hydrogen passivated defects at the Si/SiO_2 interface is 2.56 eV [26, 27]. Since this value is close to that of the stretching mode, the new version of our hot-carrier degradation model was recalibrated in a manner to employ the parameter set which corresponds to the stretching mode. In the context of

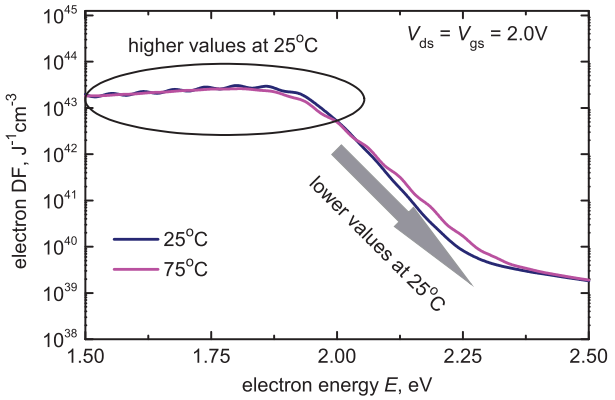

Fig. 2. The fragment of the electron DF simulated for $V_{\rm ds} = V_{\rm gs} = 2.0\,{\rm V}$ and for two different temperatures, namely for 25 and 75° C. This exemplary DF corresponds to the near-drain MOSFET area, close to the region where the carriers are hottest. One can see that for energies lower than ∼2.15 eV the DF values obtained at higher T are lower, while for higher energies the situation is reversed.

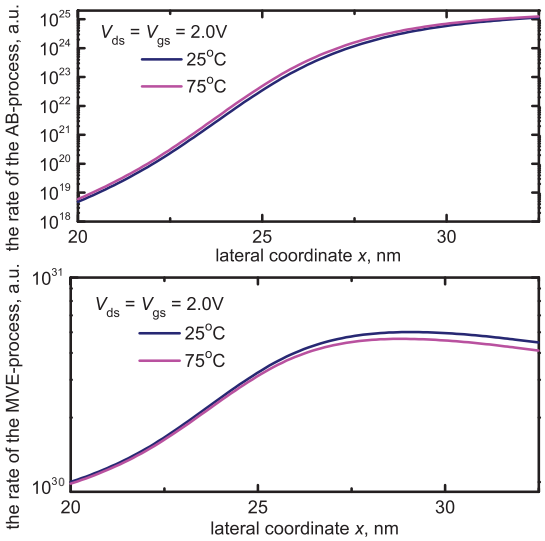

Fig. 3. The rates of the AB- and MVE-processes plotted for the near drain area of the device for 25 and 75° C. The stress voltages are $V_{\rm ds} = V_{\rm gs} = 2.0\,{\rm V}$. One can see that in the case of the AB-process the rate is higher at 75° C, while for the MVE-process the trend is reversed.

the temperature behavior of HCD, an important parameter is the vibrational life-time $\tau_{\rm e}$. Although there is a substantial number of papers focused on the calculation of this life-time, they primarily show the data in a very tight temperature range (usually for low temperatures), see [19, 25, 28], as well as [18] and references herein. Fortunately, in [20] the life-time values for both stretching and bending modes were simulated within a wide temperature range of 0 – 600 K. In our model we thus use the values published in [20], i.e. the stretching life-time at $T = 25^{\rm o}\,{\rm C}$ is $\tau_{\rm e} = 1.5\,{\rm ns}$, while for $T = 75^{\rm o}\,{\rm C}$ we employ $\tau_{\rm e} = 1.3\,{\rm ns}$.

IV. Results and Discussion

Fig. 2 shows a fragment of the electron distribution function simulated with ViennaSHE for $V_{\rm ds} = V_{\rm gs} = 2.0\,{\rm V}$ and for two different temperatures, 25 and 75° C. The DFs used for this example correspond to the most degraded drain area of the device, i.e. the place where carriers are hottest. One can see that for energies lower than ∼2.15 eV the DFs obtained at 25° C are higher than those for 75° C, while for higher energies the trend is reversed. The fact that the high-energy tails of the DF are more populated at 75° C is related to the role of electron-electron scattering which forms a characteristic hump visible in the DFs [2, 5, 9]. Since the dominant contribution to the AB-process is made by hot carriers and high-energy DF tails are more populated at 75° C, one expects that the corresponding rate will be higher at elevated temperature. Vice versa, the MVE-process is driven by colder carriers, and thus the MVE-process rate will be higher for $T = 25^{\rm o}\,{\rm C}$. This is confirmed by Fig. 3 which shows the rates for the AB-process from the bond ground state ($E_i = 0$) and the MVE-process rate simulated for $V_{\rm ds} = V_{\rm gs} = 2.0\,{\rm V}$ and two different temperatures.

To calibrate our HCD model in a manner to represent the experimental data summarized in Fig. 1 we have employed the following cross section values: $\sigma_{\rm MVE,0} = 5{\times}10^{-19}\,{\rm cm}^{-2}$ and $\sigma_{\rm AB,0} = 5{\times}10^{-18}\,{\rm cm}^{-2}$. Note that these parameters (which correspond to $E_{\rm a} = 2.56\,{\rm eV}$) are physically more reasonable than those used for the AB-process in the previous version of our model, i.e. $E_{\rm a} = 1.5\,{\rm eV}$, $\sigma_{\rm AB,0} = 2.5{\times}10^{-23}\,{\rm cm}^{-2}$. The current $\sigma_{\rm MVE,0}$ and $\sigma_{\rm AB,0}$ values ensure that the MVE-process rate is higher at $V_{\rm ds} = V_{\rm gs} = 1.8$ and 2.0 V, while the AB-mechanism dominates at $V_{\rm ds} = V_{\rm gs} = 2.2\,{\rm V}$.

Fig. 1 shows good agreement between experimental and simulated $\Delta I_{\rm dlin}(t)$ dependencies. To study the interplay between the AB- and MVE-processes in greater detail we have also simulated HCD traces neglecting the AB-process which are presented in Fig. 4. One can see that if the AB-process is ignored the distance between the $\Delta I_{\rm dlin}(t)$ curves evaluated at 25 and 75° C dramatically increases. Even in the case of $V_{\rm ds} = V_{\rm gs} = 2.2\,{\rm V}$ hot-carrier degradation is still weaker at 75° C. This is because in this artificial case hot-carrier degradation is driven by the MVE-process, the rate of which reduces with T, cf. Fig. 3.

It is important to emphasize that the vibrational life-time, which is a decreasing function of temperature, also plays a very important role in the HCD temperature behavior. In fact, a shorter life-time $\tau_{\rm e}$ means that the corresponding vibrational mode decays faster at higher T. As a result, the intermediate bond levels are less populated, and the AB-process rate from these particular levels is lower, thereby additionally weakening hot-carrier degradation at elevated temperatures. To illustrate the role of $\tau_{\rm e}(T)$ we have plotted the changes in the linear drain current for the case of $T = 75^{\rm o}\,{\rm C}$ but simulated with the same value of $\tau_{\rm e} = 1.5\,{\rm ns}$ (instead of 1.3 ns) as for 25° C. One can see that a spuriously high $\tau_{\rm e}$ value results in substantially overestimated $\Delta I_{\rm dlin}(t)$ values.

V. Conclusion

We have presented and calibrated a refined version of our physics-based model for hot-carrier degradation. The new model considers the temperature dependence of the Si-H

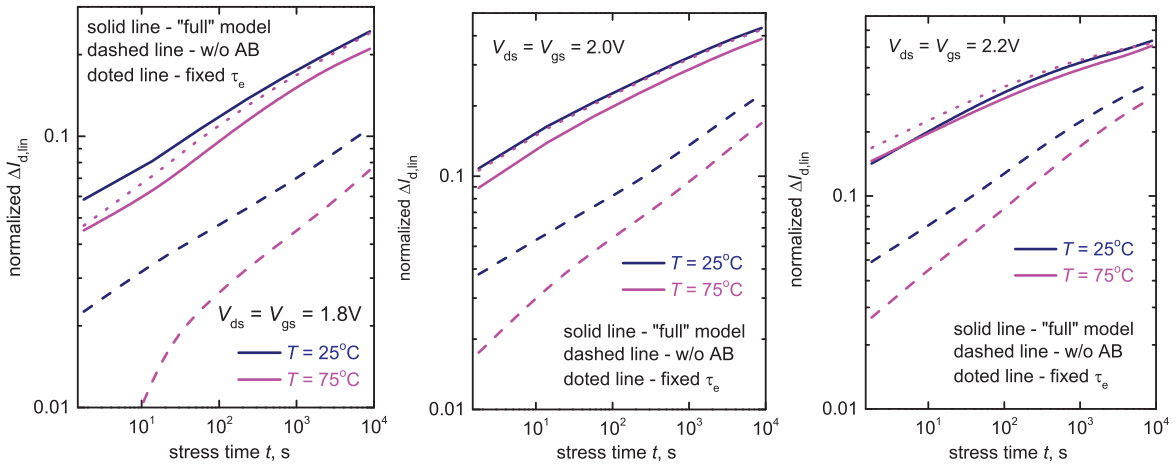

Fig. 4. The $\Delta I_{\mathrm{dlin}}(t)$ traces simulated for all combinations of V_{ds}, V_{gs} and for both temperatures with the "full" model and without the AB-process. Also for the case of T = 75° C, $\Delta I_{\mathrm{dlin}}(t)$ curves were evaluated using the same vibrational life-time as for T = 25° C, i.e. τ_{e} = 1.5 ns.

bond vibrational life-time. As opposed to previous hot-carrier degradation models, we assume that bond dissociation occurs via the stretching mode, rather than the bending mode. The stretching mode is characterized by a bond-breakage energy of ∼2.5 eV corresponding to experimental findings which report a value of 2.56 eV. With the newest version of our model we were able to represent the temperature behavior of HCD in scaled nMOSFETs with a channel length of 44 nm. In contrast to previous findings, in these short-channel transistors the linear drain current change appears to be less severe at 75° C than at 25° C.

The difference between the $\Delta I_{\mathrm{dlin}}(t)$ curves, however, was shown to decrease as stress voltages increase. At a combination of drain and gate voltages of $V_{\mathrm{ds}} = V_{\mathrm{gs}} = 2.2$ V, ΔI_{dlin} is almost the same in the whole stress time window. This behavior was explained by considering a strong coupling between the single-carrier process of Si-H bond dissociation and the multiple vibrational excitation of the bond. We have shown that the rate of the former process is higher at elevated temperature but the latter mechanism becomes weaker as the device is heated. At lower V_{ds}, V_{gs} the temperature behavior is determined by the multiple vibrational excitation process, while at higher voltages the single-carrier process starts to play a dominant role. The role of this AB-mechanism was studied by simulating the $\Delta I_{\mathrm{dlin}}(t)$ curves without the effect of the AB-process. It was shown that if the AB-mechanism is neglected the distance between the HCD traces computed at two different temperatures substantially increases.

We have also studied the role of the Si-H bond vibrational life-time, which is a decreasing function of temperature, on the HCD temperature dependence and have proven that τ_{e} is an essential model ingredient. A lower τ_{e} value (at 75° C) means that the vibrational mode decays faster, excited bond eigenstates are less populated, and the bond-breakage rate is lower, resulting thereby in suppressed HCD at higher temperatures.

Acknowledgment

The authors acknowledge support by the Austrian Science Fund (FWF), grants P23598 and P26382, and the European Community FP7 projects N° 619234 (MoRV) and 619246 (ATHENIS_3D).

References

[1] W. McMahon *et al.*, *Proc. International Conference on Modeling and Simulation of Microsystem* (2002), Vol. 1, pp. 576–579.
[2] S. Rauch *et al.*, *Proc. International Reliability Physics Symposium (IRPS), tutorial* (2010).
[3] A. Bravaix *et al.*, *Proc. International Reliability Physics Symposium (IRPS)* (2009), pp. 531–546.
[4] S. Tyaginov *et al.*, *Proc. International Integrated Reliability Workshop (IIRW)* (2012), pp. 206–215.
[5] M. Bina *et al.*, IEEE Transactions on Electron Devices **61**, 3103 (2014).
[6] S. Reggiani *et al.*, Solid-State Electronics **102**, 25 (2014).
[7] P. Sharma *et al.*, IEEE Transactions on Electron Devices **62**, 1811 (2015).
[8] S. Tyaginov *et al.*, *Proc. International Integrated Reliability Workshop (IIRW)* (2014), pp. 63–68.
[9] S. Tyaginov *et al.*, Japanese Journal of Applied Physics **54**, 04DC18 (2015).
[10] Y. Randriamihaja *et al.*, Microel. Reliab. **52**, 2513 (2012).
[11] S. Tyaginov *et al.*, *Proc. International Reliability Physics Symposium (IRPS)* (2014), pp. XT.16–1–16–8.
[12] F.-C. Hsu *et al.*, IEEE Electron Device Letters **5**, 148 (1984).
[13] M. Song *et al.*, IEEE Transactions Electron Devices **44**, 268 (1997).
[14] P. Childs *et al.*, Journal of Applied Physics **79**, 222 (1996).
[15] S. Rauch *et al.*, IEEE Electron Dev. Lett. **19**, 463 (1998).
[16] E. Amat *et al.*, Microelectronics Engineering **87**, 47 (2010).
[17] A. Bravaix *et al.*, *Proc. International Electron Devices Meeting (IEDM)* (2011), pp. 622–625.
[18] C. Guerin *et al.*, Journal of Applied Physics **105**, 114513 (2009).
[19] G. Lüpke *et al.*, Physical Review Letters **88**, 135501 (2002).
[20] I. Andrianov *et al.*, The Journal of Chemical Physics **124**, 034710 (2006).
[21] *http://viennashe.sourceforge.net/*, 2014.
[22] M. Bina *et al.*, *Proc. International Electron Devices Meeting (IEDM)* (2012), pp. 713–716.
[23] J. McPherson, *Proc. International Reliability Physics Symposium (IRPS)* (2007), pp. 209–216.
[24] B. Persson *et al.*, Surface Science **390**, 45 (1997).
[25] M. Budde *et al.*, Phys. Rev. Lett. **87**, 1455 (2001).
[26] K. Brower, Physical Review B **42**, 3444 (1990).
[27] A. Stesmans, Appl. Phys. Lett. **68**, 2076 (1996).
[28] R. Honke *et al.*, Physical Review B **59**, 10996 (1999).